Computer Modeling in Engineering & Sciences

Tech Science Press

Doi:10.32604/cmes.2025.069277

ARTICLE

Investigating the Role of Antimalarial Treatment and Mosquito Nets in Malaria Transmission and Control through Mathematical Modeling

Azhar Iqbal Kashif Butt[1,*], Tariq Ismaeel[2,*], Sara Khan[2], Muhammad Imran[3], Waheed Ahmad[2], Ismail Abdulrashid[4] and Muhammad Sajid Riaz[5]

[1]Department of Mathematics and Statistics, College of Science, King Faisal University, Al-Ahsa, 31982, Saudi Arabia
[2]Department of Mathematics, Government College University, Lahore, 54000, Pakistan
[3]Tandy School of Computer Science, University of Tulsa, Tulsa, OK 74104, USA
[4]School of Finance and Operations Management, University of Tulsa, Tulsa, OK 74104, USA
[5]Polytechnic Institute, University of Oklahoma, Tulsa, OK 74135, USA

*Corresponding Authors: Azhar Iqbal Kashif Butt. Email: aikhan@kfu.edu.sa; Tariq Ismaeel. Email: tariqismaeel@gcu.edu.pk

Received: 19 June 2025; Accepted: 20 August 2025; Published: 30 September 2025

ABSTRACT: Malaria is a significant global health challenge. This devastating disease continues to affect millions, especially in tropical regions. It is caused by Plasmodium parasites transmitted by female Anopheles mosquitoes. This study introduces a nonlinear mathematical model for examining the transmission dynamics of malaria, incorporating both human and mosquito populations. We aim to identify the key factors driving the endemic spread of malaria, determine feasible solutions, and provide insights that lead to the development of effective prevention and management strategies. We derive the basic reproductive number employing the next-generation matrix approach and identify the disease-free and endemic equilibrium points. Stability analyses indicate that the disease-free equilibrium is locally and globally stable when the reproductive number is below one, whereas an endemic equilibrium persists when this threshold is exceeded. Sensitivity analysis identifies the most influential mosquito-related parameters, particularly the bite rate and mosquito mortality, in controlling the spread of malaria. Furthermore, we extend our model to include a treatment compartment and three disease-preventive control variables such as antimalaria drug treatments, use of larvicides, and the use of insecticide-treated mosquito nets for optimal control analysis. The results show that optimal use of mosquito nets, use of larvicides for mosquito population control, and treatment can lower the basic reproduction number and control malaria transmission with minimal intervention costs. The analysis of disease control strategies and findings offers valuable information for policymakers in designing cost-effective strategies to combat malaria.

KEYWORDS: Malaria; mathematical modeling; optimal control; mosquito nets; anti-malaria drugs; stability and sensitivity analysis

Mathematics Subject Classification: 34H05, 49K15, 49K40

1 Introduction

Malaria is a contagious disease caused by Plasmodium parasites, mainly transmitted to humans through the bite of a female mosquito [1]. Although there has been significant progress in decreasing the number of malaria cases worldwide, the disease continues to pose an important public health challenge, especially in tropical and subtropical regions. The groups at risk include children under the age of five, pregnant women, and travelers who lack immunity [1,2]. Travelers from countries without local malaria transmission are at

significant risk of contracting malaria and its consequences when traveling abroad, as they lack immunity. Additionally, individuals who leave malaria-endemic countries and immigrate to malaria-free nations are also at risk when they return to their home countries to visit friends and family, as their immunity wanes or becomes nonexistent. However, Sub-Saharan Africa remains the most vulnerable region, representing a significantly high share of deaths attributed to malaria [3].

Female mosquitoes that transmit disease have salivary glands that contain sporozoites. In the human body, these sporozoites develop into two forms: erythrocytic and hepatocyte schizogony. During the hepatocyte phase, the sporozoite transforms into a hypnozoite, a dormant form, which later develops into a schizont [4]. The schizont undergoes rapid cell division, producing merozoites that infect red blood cells. Meanwhile, hypnozoites can remain dormant for an extended period. The merozoites produced in the liver invade red blood cells, thereby sustaining the cycle of infection [5]. Trophozoites form and associate with merozoites, developing into blood schizonts that produce merozoites to infect new red blood cells. In some plasmodium parasites, hypnozoites develop into liver schizonts that burst, releasing a large number of merozoites after 8 to 10 months. The number of sporozoites injected by mosquitoes into humans is a crucial factor in the recurrence of malaria [6].

To mitigate the impact of malaria on the global population, various scientific initiatives have been undertaken, including the development of mathematical models [7,8]. The SEIR model, introduced by Kermack and McKendrick, has been widely adopted for modeling malaria transmission [9–11]. Since then, numerous mathematical models have been developed to combat malaria and reduce its global mortality rate [12–14]. However, predicting the severity of malaria remains a challenging task despite these efforts. As climate change awareness grows, it's essential to recognize the significant impact of climatic and environmental conditions on the spread and transmission of vector-borne diseases [15]. Environmental factors like temperature, rainfall, humidity, wind speed, and daylight duration play a crucial role in shaping the seasonal and daily rhythms of mosquito populations, influencing their ecological and behavioral aspects [16].

Mathematical modeling has become a powerful tool in understanding the transmission dynamics of malaria [17–21]. In [22], the primary focus was on the development of a mathematical model and the evaluation of two disease control strategies: human precautions and mosquito sprays. The study determined that the system achieves a disease-free state when at least 40% of susceptible humans undertake the necessary precautions. In another study [23], the authors proposed an effective disease control approach known as awareness-based intervention, which utilizes media for malaria management. The model incorporates time-dependent control measures for treatment, insecticides, and social media initiatives to minimize the costs associated with malaria control. A new mathematical model using partial differential equations was developed for malaria in [24]. The authors studied the effectiveness of spraying in malaria control and found that uniform spraying produced comparable results to a non-spatial model.

Most mathematical models overlook the mosquito life cycle, excluding eggs, larvae, and pupae from the transmission cycle. While this simplification is helpful, it leads to a significant limitation: these models often struggle to accurately predict the magnitude of malaria in regions where it is most prevalent. To comprehensively understand the complex processes driving malaria transmission and develop more accurate predictive models, it is essential to consider the mosquito life cycle and the impacts of seasonality [25]. Moulay et al. [26] recently developed a mathematical model that simulates the dynamics of mosquito populations, incorporating the self-regulatory mechanisms of the egg and larval stages. They identified a threshold that plays a crucial role in controlling mosquito population growth. However, these models often overlook important factors like the life cycle of mosquitoes and variations in the environment. This can lead to inaccuracies in predicting the severity of the disease, particularly in areas where malaria is widespread.

In comparison to earlier models [22–26] that either assume a constant mosquito population or neglect the impact of treatments, this study addresses these shortcomings by integrating the dynamics of mosquito populations and seasonal variations into a non-linear mathematical model. It also presents a more comprehensive model that incorporates both symptomatic and asymptomatic human infections, considers the different stages of the mosquito life cycle, and integrates treatment effects with vector control. This approach improves realism and facilitates the examination of integrated control strategies. Overall, the combination of stability analysis, detailed compartmental dynamics, and optimal control within realistic constraints represents a significant advancement that differentiates it from existing approaches in both scope and suitability. We will explore the most efficient approaches to managing the disease, emphasizing the utilization of anti-malaria medications, vector control methods to reduce mosquito populations, and the use of mosquito nets.

The sections of the article are arranged as follows. Section 2 outlines the formulation of the model, which divides human and mosquito populations into different compartments and uses a set of nonlinear ordinary differential equations (ODEs) to represent the spread of the disease. In Section 3, we present theoretical findings, including the existence, uniqueness, positivity, and boundedness of the model's solutions. The stability analysis of disease-free equilibrium (DFE), and endemic equilibrium (EE) with respect to reproduction number R_0 is also presented in this section. Section 4 focuses on sensitivity analysis, identifying the most crucial parameters influencing R_0. This section also uses numerical simulations to demonstrate the system's dynamics under various R_0 scenarios, illustrating disease-free and endemic conditions. Section 5 expands the model to incorporate optimal control strategies, including the use of anti-malaria drugs, vector population control strategies, and mosquito nets. Section 6 formulates and solves an optimal control problem using Pontryagin's Maximum Principle to minimize both malaria transmission and intervention costs. The paper concludes by identifying the most effective strategies for malaria control, supported by numerical results.

2 Mathematical Modeling of Malaria

We develop an extended SEIR-based mathematical model that incorporates asymptomatic human cases and vector populations, capturing the complex dynamics of malaria transmission more effectively than classical models. The SEIR type models are particularly effective for modeling malaria because they include a latency period in both human and mosquito populations. The model will analyze how human and mosquito populations change over time, with humans represented as $N_h(t)$ and mosquitoes as $N_v(t)$. We categorize mosquitoes into two populations: immature and mature. The mature mosquito population is divided into three compartments: susceptible (S_v), exposed (E_v), and infected (I_v). Similarly, the human population is divided into five compartments: susceptible (S_h), exposed (E_h), infected (I_h), asymptomatic (A_h), and recovered (R_h).

The infection period of mosquitoes is directly correlated with their relatively short life. Therefore, our model focuses exclusively on mature mosquitoes, as their maturity aligns with their infection period. At any given time t, the combined population consists of mature mosquitoes and humans, represented by:

$$N_v(t) = S_v(t) + E_v(t) + I_v(t), \tag{1}$$

and

$$N_h(t) = S_h(t) + E_h(t) + I_h(t) + A_h(t) + R_h(t). \tag{2}$$

The growth rate of mosquitoes is represented by Λ_v. When an uninfected female mosquito bites a human infected with a virus or parasite, the mosquito becomes a carrier of the infectious agent. The force of infection in this case is represented by:

$$\frac{\sigma c S_v I_h}{N_h},$$

and hence the susceptible mosquitoes move to the exposed class at this rate. The exposed mosquitoes become infectious at the rate ν_v. The mosquito population dies naturally at the rate μ_v.

The susceptible humans are recruited at a constant birth rate Λ_h. Once the infected mosquito bites a susceptible human, it can transmit the parasite to that human, potentially resulting in an infection. Thus, susceptible humans are exposed to the virus at the rate given as:

$$\frac{\sigma b S_h I_v}{N_h}.$$

The humans exposed to the virus become infectious, which can further be divided into two subgroups: symptomatic and asymptomatic. The rate at which symptomatic individuals develop symptoms is denoted by β_1, and the rate at which asymptomatic individuals become infectious is denoted by β_2. After individuals recover from infection, they gain immunity from the disease. Both symptomatic and asymptomatic individuals move to the recovered class, represented as R_h, after acquiring immunity at rates θ and γ, respectively. The rate of natural death is denoted by μ_h, while the rate of death due to the disease is denoted by δ_h. The above considerations are depicted by the flow diagram shown in Fig. 1.

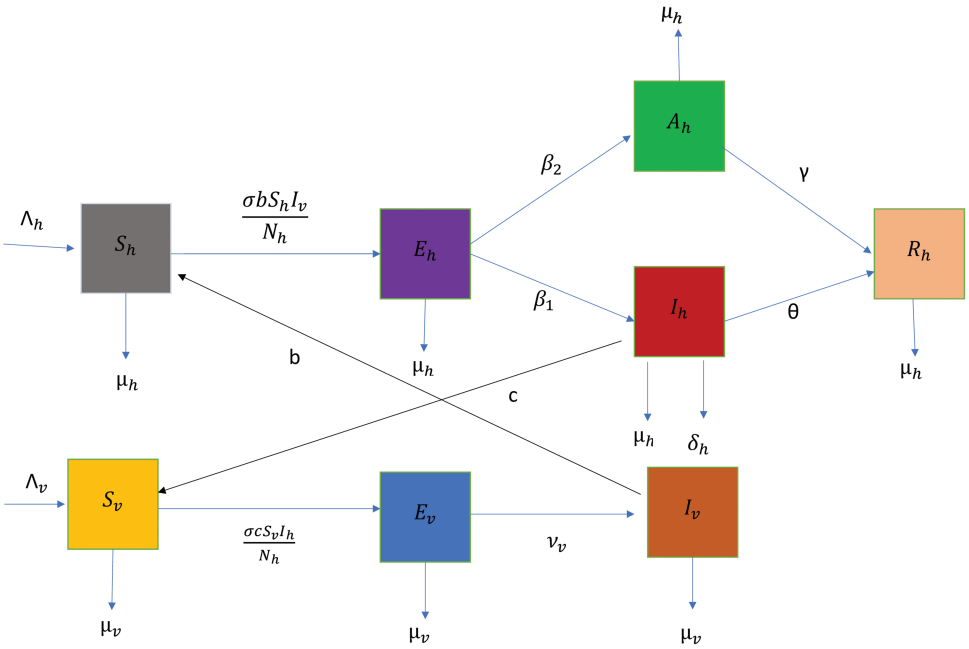

Figure 1: Diagram showing the transmission of disease through the compartments

The malaria parasite transmission flow diagram is transformed into the following system of nonlinear ODEs:

$$\frac{dS_h}{dt} = \Lambda_h - \frac{\sigma b S_h I_v}{N_h} - \mu_h S_h, \tag{3a}$$

$$\frac{dE_h}{dt} = \frac{\sigma b S_h I_v}{N_h} - (\beta_1 + \beta_2 + \mu_h) E_h, \tag{3b}$$

$$\frac{dI_h}{dt} = \beta_1 E_h - (\theta + \mu_h + \delta_h) I_h, \tag{3c}$$

$$\frac{dA_h}{dt} = \beta_2 E_h - (\mu_h + \gamma) A_h, \tag{3d}$$

$$\frac{dR_h}{dt} = \theta I_h + \gamma A_h - \mu_h R_h, \tag{3e}$$

$$\frac{dS_v}{dt} = \Lambda_v - \frac{\sigma c S_v I_h}{N_h} - \mu_v S_v, \tag{3f}$$

$$\frac{dE_v}{dt} = \frac{\sigma c S_v I_h}{N_h} - (\nu_v + \mu_v) E_v, \tag{3g}$$

$$\frac{dI_v}{dt} = \nu_v E_v - \mu_v I_v, \tag{3h}$$

with initial conditions that are non-negative, i.e.,

$$\begin{aligned} &S_h(0) = S_{h0} > 0, \quad E_h(0) = E_{h0} \geq 0, \quad I_h(0) = I_{h0} \geq 0, \quad A_h(0) = A_{h0} \geq 0, \\ &R_h(0) = R_{h0} \geq 0, \quad S_v(0) = S_{v0} > 0, \quad E_v(0) = E_{v0} \geq 0, \quad I_v(0) = I_{v0} \geq 0. \end{aligned} \tag{3i}$$

Table 1 presents the model parameters' descriptions and values. In compact form, we put the model (3) as follows:

$$\frac{d\Psi}{dt} = H(\Psi(t)), \quad \Psi(0) = \Psi_0, \ 0 < t < t_f < \infty, \tag{4}$$

where $\Psi(t) : [0, t_f] \to R_+^8$ and $H : R_+^8 \to R_+^8$ are function defined by:

$$\Psi(t) = (S_h(t), E_h(t), I_h(t), A_h(t), R_h(t), S_v(t), E_v(t), I_v(t))^T,$$

with

$$\Psi_0 = (S_h(0), E_h(0), I_h(0), A_h(0), R_h(0), S_v(0), E_v(0), I_v(0))^T,$$

and

$$H(\Psi(t)) = \begin{pmatrix} H_1 \\ H_2 \\ H_3 \\ H_4 \\ H_5 \\ H_6 \\ H_7 \\ H_8 \end{pmatrix} = \begin{pmatrix} \Lambda_h - \dfrac{\sigma b S_h I_v}{N_h} - \mu_h S_h \\ \dfrac{\sigma b S_h I_v}{N_h} - (\beta_1 + \beta_2 + \mu_h) E_h \\ \beta_1 E_h - (\theta + \mu_h + \delta_h) I_h \\ \beta_2 E_h - (\mu_h + \gamma) A_h \\ \theta I_h + \gamma A_h - \mu_h R_h \\ \Lambda_v - \dfrac{\sigma c S_v I_h}{N_h} - \mu_v S_v \\ \dfrac{\sigma c S_v I_h}{N_h} - (\nu_v + \mu_v) E_v \\ \nu_v E_v - \mu_v I_v \end{pmatrix}.$$

Table 1: Values for parameters along with their descriptions

Parameters	Description	Disease-free	Endemic state
Λ_v	Constant mosquito birth rate	45	45
σ	The average mosquito bite rate per person	0.42	1.94
c	Disease transmission probability from infectious vectors to susceptible humans	0.50	0.44
μ_v	The natural mortality rate of mosquitoes	0.015	0.015
ν_v	The period of external incubation for mosquitoes	0.423	0.423
Λ_h	Consistent human rate	23	23
b	Disease transmission probability from infectious humans to susceptible vectors	0.022	0.022
δ_h	The mortality rate caused by malaria in humans	0.038	0.038
β_1	The likelihood of contracting clinical infection	1.08	1.08
β_2	The likelihood of asymptomatic infection	1.13	1.13
γ	The rate of asymptomatic infections	0.29	0.29
θ	The clinical disease rate	0.359	0.359
μ_h	The human mortality rate	0.029	0.029

3 Theoretical Results

In this section, we present the main theoretical results, demonstrating the physical viability of the proposed mathematical model and its potential for further exploration in numerical simulations. We establish the uniqueness of the solution of the model (3) and verify that the solution of each state equation remains positive and bounded for all $t \geq 0$. Furthermore, we determine the equilibrium points and the basic reproduction number ($\mathcal{R}_0$) to assess the local and global stability of the proposed model at these points.

3.1 Positivity and Boundedness of the Solutions

We aim to establish that the variable $\Psi = (S_h, E_h, I_h, A_h, R_h, S_v, E_v, I_v)$ remains positive and bounded for $t \geq 0$ in the analysis of the fundamental characteristics of the malaria transmission model.

Theorem 1: *The solution* $\Psi = (S_v, E_v, I_v, S_h, E_h, I_h, A_h, R_h)$ *to the model has been shown to maintain positivity under consideration of the initial condition provided in Eq. (3i).*

Proof: The Eq. (3f) can be rewritten as:

$$\frac{dS_v}{dt} + \left(\frac{\sigma c I_h}{N_h} + \mu_v\right) S_v = \Lambda_v, \tag{5}$$

or

$$\frac{dS_v}{dt} + (\Phi(t) + \mu_v)\, S_v = \Lambda_v, \tag{6}$$

where

$$\Phi(t) = \frac{\sigma c I_h}{N_h}.$$

The differential Eq. (6) yields us an integrated factor $exp\left(\mu_v t + \int_0^t \Phi(x)dx\right)$. As a result, the Eq. (6) can be written as:

$$\frac{d}{dt}\left[exp\left(\mu_v t + \int_0^t \Phi(x)dx\right)S_v\right] = \Lambda_v\, exp\left(\mu_v t + \int_0^t \Phi(x)dx\right).$$

Integrating the above equation over the interval $[0, \tau]$, where $\tau = \max\{t > 0,\ \Psi(t) > 0\}$, we determine:

$$S_v(\tau)\, exp\left(\mu_v \tau + \int_0^\tau \Phi(x)dx\right) - S_v(0) = \Lambda_v \int_0^\tau exp\left(\mu_v t + \int_0^t \Phi(x)dx\right)dt.$$

After simplification, we obtain the following expression for S_v.

$$\begin{aligned} S_v(\tau) = {} & S_v(0)\, exp\left(-(\mu_h \tau + \int_0^\tau \Phi(x)dx)\right) \\ & + exp\left(-(\mu_v \tau + \int_0^\tau \Phi(x)dx)\right)\left(\Lambda_v \int_0^\tau exp\left(\mu_v t + \int_0^t \Phi(x)dx\right)dt\right). \end{aligned} \tag{7}$$

Given $S_v(0) \geq 0$, Eq. (7) implies that $S_v(t) > 0$ for all $t \in [0, \tau]$. Following a similar procedure, the positivity for all other variables can be demonstrated. □

Theorem 2: *The solution* $\Psi(t)$ *for the malaria disease model (3) is bounded for* $t \geq 0$.

Proof: Differentiating Eqs. (1) and (2) with respect to time t and then incorporating the equations of disease model (3), we obtain the following ODEs for total vector and human populations.

$$\frac{dN_v}{dt} = \Lambda_v - \mu_v N_v, \tag{8}$$

and

$$\frac{dN_h}{dt} = \Lambda_h - \delta_h I_h - \mu_h N_h \leq \Lambda_h - \mu_h N_h, \tag{9}$$

with

$$N_v(0) = S_v(0) + E_v(0) + I_v(0),$$

and

$$N_h(0) = S_h(0) + E_h(0) + I_h(0) + A_h(0) + R_h(0).$$

Suppose for any given initial condition, if

$$N_v(0) \leq \frac{\Lambda_v}{\mu_v}, \tag{10}$$

then

$$\frac{dN_v}{dt} \leq \Lambda_v - \mu_v N_v.$$

Similarly if

$$N_h(0) \leq \frac{\Lambda_h}{\mu_h}, \tag{11}$$

then

$$\frac{dN_h}{dt} \leq \Lambda_h - \mu_h N_h.$$

We employ the Grönwall's inequality to determine the following solutions.

$$N_v(t) \leq \frac{\Lambda_v}{\mu_v} + \left(N_v(0) - \frac{\Lambda_v}{\mu_v}\right) exp\left((-\mu_v)t\right),$$

and

$$N_h(t) \leq \frac{\Lambda_h}{\mu_h} + \left(N_h(0) - \frac{\Lambda_h}{\mu_h}\right) exp\left((-\mu_h)t\right).$$

This implies that

$$N_v(t) \leq \frac{\Lambda_v}{\mu_v}, \text{ for all } t \geq 0,$$

and

$$N_h(t) \leq \frac{\Lambda_h}{\mu_h}, \text{ for all } t \geq 0.$$

Thus, we can write the following inequalities.

$$\lim_{t\to\infty} N_v(t) \le \frac{\Lambda_v}{\mu_v},$$
$$\lim_{t\to\infty} N_h(t) \le \frac{\Lambda_h}{\mu_h},$$

which proves the boundedness of $\Psi(t)$ for every $t \ge 0$. □

As a result of the above two theorems, the feasible region for the proposed model (3) is defined as follows.

$$\Delta = \left\{\Psi \in R_+^8\ 0 < N_v \le \frac{\Lambda_v}{\mu_v},\ 0 < N_h \le \frac{\Lambda_h}{\mu_h},\ 0 \le t \le \tau < \infty\right\}.$$

3.2 Existence and Uniqueness

To demonstrate the existence and uniqueness of the solutions of the disease model (3), we present the following foundational results of [27,28].

Theorem 3: *Consider the domain* $D = \{(t, v_1, \ldots, v_m) | a \le t \le b, -\infty < v_k < \infty,$ *for each* $k = 1, 2, \ldots, m\}$. *Suppose that each function* $\mathcal{G}_k(1, v_1, \ldots, v_m)$, *for* $k = 1, \ldots, m$, *is continuous and satisfies the Lipschitz condition on D. Then, the system:*

$$\frac{dv}{dt} = \mathcal{G}(t, v),\ v(a) = v_0,$$

where $v = (v_1, \ldots, v_m)^T$, $v_0 = ((v_0)_1, \ldots, (v_0)_m)^T$, $\mathcal{G} = (\mathcal{G}_1, \ldots \mathcal{G}_m)^T$ *has a unique solution v for* $t \in [a, b]$.

Theorem 4: *If* $\mathcal{G}(t, v)$ *and* $\frac{\partial \mathcal{G}}{\partial v_k}$ *are in* $C(D)$ *and if*

$$\left|\frac{\partial \mathcal{G}}{\partial v_k}\right| < \mathcal{M},$$

then for $\mathcal{M} > 0$, $\mathcal{G}$ *satisfies the Lipschitz condition on D for each k = 1, . . ., m in D.*

We now introduce the theorem that establishes the existence of a unique solution for IVP (4).

Theorem 5: *Assume that the domain for the problem (4) is* $\Delta \subset D$. *The system (4) has a unique solution bounded in* Δ *if H satisfies the Lipschitz condition on* Δ.

Proof: Here, the function $H(\Psi(t))$ and its partial derivative are continuous since the state variable $\Psi(t)$ is continuously differentiable for $0 \le t \le \tau < \infty$. Additionally, Theorems 1 and 2 state that $H(\Psi(t))$ is bounded. To demonstrate Lipschitz's condition on Δ, all that is required is proving the boundedness of the derivatives $\frac{\partial H_i}{\partial \Psi_k}$, where $i, k = 1, \ldots, 8$.

$$\left|\frac{\partial H_1}{\partial S_h}\right| = \left| -\left(\frac{\sigma c I_v}{N_h} + \mu_h\right)\right| \le \mathcal{M} < \infty,$$
$$\left|\frac{\partial H_1}{\partial I_v}\right| = \left| -\left(\frac{\sigma c S_h}{N_h}\right)\right| \le \mathcal{M} < \infty,$$

$$\left|\frac{\partial H_2}{\partial S_h}\right| = \left|\left(\frac{\sigma c I_v}{N_h}\right)\right| \leq \mathcal{M} < \infty,$$
$$\left|\frac{\partial H_2}{\partial I_v}\right| = \left|\left(\frac{\sigma c S_h}{N_h}\right)\right| \leq \mathcal{M} < \infty,$$
$$\left|\frac{\partial H_2}{\partial E_h}\right| = |-(\beta_1 + \beta_3 + \mu_h)| \leq \mathcal{M} < \infty,$$
$$\left|\frac{\partial H_3}{\partial E_h}\right| = |(\beta_1)| \leq \mathcal{M} < \infty,$$
$$\left|\frac{\partial H_3}{\partial I_h}\right| = |-(\theta + \delta_h + \mu_h)| \leq \mathcal{M} < \infty,$$
$$\left|\frac{\partial H_4}{\partial E_h}\right| = |(\beta_2)| \leq \mathcal{M} < \infty,$$
$$\left|\frac{\partial H_4}{\partial A_h}\right| = |-(\gamma + \mu_h)| \leq \mathcal{M} < \infty,$$
$$\left|\frac{\partial H_5}{\partial I_h}\right| = |(\theta)| \leq \mathcal{M} < \infty,$$
$$\left|\frac{\partial H_5}{\partial A_h}\right| = |(\gamma)| \leq \mathcal{M} < \infty,$$
$$\left|\frac{\partial H_5}{\partial R_h}\right| = |-(\mu_h)| \leq \mathcal{M} < \infty.$$
$$\left|\frac{\partial H_6}{\partial S_v}\right| = \left|-\left(\frac{\sigma c I_h}{N_h} + \mu_v\right)\right| \leq \mathcal{M} < \infty,$$
$$\left|\frac{\partial H_6}{\partial I_h}\right| = \left|\left(\frac{\sigma c S_v}{N_h}\right)\right| \leq \mathcal{M} < \infty,$$
$$\left|\frac{\partial H_7}{\partial I_h}\right| = \left|\left(\frac{\sigma c S_v}{N_h}\right)\right| \leq \mathcal{M} < \infty,$$
$$\left|\frac{\partial H_7}{\partial S_v}\right| = \left|\left(\frac{\sigma c I_h}{N_h}\right)\right| \leq \mathcal{M} < \infty,$$
$$\left|\frac{\partial H_7}{\partial E_v}\right| = |-(v_v + \mu_v)| \leq \mathcal{M} < \infty,$$
$$\left|\frac{\partial H_8}{\partial I_v}\right| = |-(\mu_v)| \leq \mathcal{M} < \infty,$$
$$\left|\frac{\partial H_8}{\partial E_v}\right| = |(v_v)| \leq \mathcal{M} < \infty,$$

All other first-order derivatives are equal to zero, i.e.,

$$\left|\frac{\partial H_i}{\partial \Psi_k}\right| = 0 < \mathcal{M} < \infty.$$

Here $\mathcal{M} = \bar{k}\bar{\mathcal{M}}$ where $\bar{k} > 0$ is the largest value of model parameters and $\bar{\mathcal{M}} = max\{\mathcal{M}_1, \ldots, \mathcal{M}_8\}$. Here, $\mathcal{M}_1, \mathcal{M}_2, \ldots, \mathcal{M}_8$ are respectively the upper bounds for each of the state variables $\Psi_k,\ k = 1, 2, \ldots, 8$.

Thus,

$$\left|\frac{\partial H_i}{\partial \Psi_k}\right| \leq \mathcal{M},\ \forall i, k = 1, \ldots 8.$$

This proves the existence of a unique solution of the disease model (4). □

3.3 Equilibrium Points

We determine the Disease-Free Equilibrium (DFE) point by setting $I_h = 0$ and $I_v = 0$ in the steady-state equation of the model (3). We solve the steady-state equations to find the following DFE point.

$$E_0 = \left(S_h^0, E_h^0, I_h^0, A_h^0, R_h^0, S_v^0, E_v^0, I_v^0\right) = \left(\frac{\Lambda_h}{\mu_h}, 0, 0, 0, 0, \frac{\Lambda_v}{\mu_v}, 0, 0\right). \tag{12}$$

The endemic equilibrium point represents a stable state in which the disease continues to persist and circulate within the population with a constant number of infected individuals who coexist within the population. In this scenario, the disease persists in both the mosquito and human populations, which means $I_v \neq 0$ and $I_h \neq 0$. To determine the endemic equilibrium (EE) point, we solve the steady-state equations of the model (3) and determine the following EE point.

$$E_1 = (S_h^1, E_h^1, I_h^1, A_h^1, R_h^1, S_v^1, E_v^1, I_v^1), \tag{13}$$

where

$$S_h^1 = \left[\frac{\Lambda_h}{(\lambda_h^1 + \mu_h)}\right],$$

$$E_h^1 = \left[\frac{\lambda_h^1 \Lambda_h}{k_1(\lambda_h^1 + \mu_h)}\right],$$

$$I_h^1 = \left[\frac{\beta_1 \lambda_h^1 \Lambda_h}{k_1 k_2(\lambda_h^1 + \mu_h)}\right],$$

$$A_h^1 = \left[\frac{\beta_1 \beta_2 \lambda_h^1 \Lambda_h}{k_1 k_2 k_3(\lambda_h^1 + \mu_h)}\right],$$

$$R_h^1 = \left[\frac{\beta_1 \lambda_h^1 \Lambda_h(\theta k_3 + \gamma \beta_2)}{k_1 k_2 k_3 \mu_h(\lambda_h^1 + \mu_h)}\right],$$

$$S_v^1 = \left[\frac{\Lambda_v}{(\lambda_v^1 + \mu_v)}\right],$$

$$E_v^1 = \left[\frac{\lambda_v^1 \Lambda_v}{k_4(\lambda_v^1 + \mu_v)}\right],$$

$$I_v^1 = \left[\frac{\nu_v \lambda_v^1 \Lambda_v}{k_4 \mu_v(\lambda_v^1 + \mu_v)}\right],$$

and

$$k_1 = (\beta_1 + \beta_2 + \mu_h),\ k_2 = (\mu_h + \delta_h + \theta),\ k_3 = (\mu_h + \gamma),\ k_4 = (\nu_v + \mu_v),$$

$$\lambda_v^1 = \frac{\sigma c I_h^1}{N_h},\ \lambda_h^1 = \frac{\sigma b I_v^1}{N_h}.$$

3.4 Reproduction Number

The reproduction number $\mathcal{R}_0$ is a crucial mathematical statistic that is used to assess the spread of a disease. The disease will spread when $\mathcal{R}_0 > 1$, while $\mathcal{R}_0 < 1$ indicates that the disease will eventually die out.

The next-generation matrix approach, introduced by Diekmann and Heesterbeek in 1970 [29,30], is widely used to calculate $\mathcal{R}_0$. This approach defines $\mathcal{R}_0$ as the spectral radius of the product of two matrices: F, the Jacobian of the new infection rate, and V^{-1}, the inverse of the Jacobian of the remaining transition terms in the disease spread equation. In simpler terms, $\mathcal{R}_0$ is the largest absolute eigenvalue of the next-generation matrix FV^{-1}, which represents the potential for the spread of the disease.

To determine $\mathcal{R}_0$, we analyze the equations for infectious states in both vector and host populations $(E_h, I_h, A_h, E_v, I_v)$ and extract the matrices $\mathcal{F}$ and $\mathcal{V}$ to compute the next-generation matrix FV^{-1}. The matrices $\mathcal{F}$ and $\mathcal{V}$ are given as follows.

$$\mathcal{F} = \begin{pmatrix} \frac{\sigma b S_h I_v}{N_h} \\ 0 \\ 0 \\ \frac{\sigma c S_v I_h}{N_h} \\ 0 \end{pmatrix}, \quad \mathcal{V} = \begin{pmatrix} (\beta_1 + \beta_2 + \mu_h) E_h \\ -\beta_1 E_h + (\theta + \mu_h + \delta_h) I_h \\ -\beta_2 E_h + (\gamma + \mu_h) A_h \\ (\nu_v + \mu_v) E_v \\ -\nu_v E_v + \mu_v I_v \end{pmatrix}.$$

The jacobian matrices F and V are then determined as follows:

$$F = \left(\frac{\partial \mathcal{F}_i}{\partial y_i} \right)_{E_0}, \quad i = 1, 2, 3, 4, 5,$$

$$V = \left(\frac{\partial \mathcal{V}_i}{\partial y_i} \right)_{E_0}, \quad i = 1, 2, 3, 4, 5,$$

where $(y_1, y_2, y_3, y_4, y_5) = (E_h, I_h, A_h, E_v, I_v)$.

Thus, $\mathcal{R}_0$, representing the spectral radius of FV^{-1}, is given as:

$$\mathcal{R}_0 = \frac{\sigma c \Lambda_v \mu_h \beta_1}{\Lambda_h \mu_v (\theta + \mu_h + \delta_h)(\beta_1 + \beta_2 + \mu_h)}. \tag{14}$$

The reproduction number, $\mathcal{R}_0$, determines the transmissibility of a disease. If $\mathcal{R}_0$ is greater than one, an outbreak will occur, and the disease will spread. On the other hand, if $\mathcal{R}_0$ is less than one, the disease will decline and eventually die out. The threshold value of $\mathcal{R}_0 = 1$ marks the tipping point, where the disease is neither spreading nor declining.

3.5 Stability Characterization of Model

This section investigates the stability of the malaria mathematical model, analyzing both local and global stability at the equilibrium points of DFE and EE.

3.5.1 Evaluation of Local Stability

To evaluate the local stability of the model at the DFE point, the Jacobian matrix is calculated and evaluated at E_0, i.e.,

$$J_{E_0} = \begin{pmatrix} -\mu_h & 0 & 0 & 0 & 0 & 0 & 0 & -\sigma b \\ 0 & -k_1 & 0 & 0 & 0 & 0 & 0 & \sigma b \\ 0 & \beta_1 & -k_2 & 0 & 0 & 0 & 0 & 0 \\ 0 & \beta_2 & 0 & -k_3 & 0 & 0 & 0 & 0 \\ 0 & 0 & \theta & \gamma & -\mu_h & 0 & 0 & 0 \\ 0 & 0 & -\frac{\sigma c \Lambda_v \mu_h}{\mu_v \Lambda_h} & 0 & 0 & -\mu_v & 0 & 0 \\ 0 & 0 & \frac{\sigma c \Lambda_v \mu_h}{\mu_v \Lambda_h} & 0 & 0 & 0 & -k_4 & 0 \\ 0 & 0 & 0 & 0 & 0 & 0 & \nu_v & -\mu_v \end{pmatrix}. \tag{15}$$

We introduce the following theorem to analyze the local stability of model (3) at the DFE point E_0.

Theorem 6: *State model (3) is locally asymptotically stable at E_0 when $\bar{\mathcal{R}}_0 < 1$, and is not stable for $\bar{\mathcal{R}}_0 > 1$.*

Proof: The Jacobian matrix (15) has the following eigenvalues.

$$\lambda_1 = -\mu_h$$
$$\lambda_2 = -\mu_h$$
$$\lambda_3 = -k_1$$
$$\lambda_4 = -k_2$$
$$\lambda_5 = -k_3$$
$$\lambda_6 = -\mu_v$$
$$\lambda_7 = -k_4$$
$$\lambda_8 = -\mu_v(1-\bar{\mathcal{R}}_0).$$

The eigenvalues (λ_1 to λ_8) are all negative when $\bar{\mathcal{R}}_0 < 1$, indicating local asymptotic stability at E_0, where $\bar{\mathcal{R}}_0 = \dfrac{\sigma \nu_v b}{\mu_v(\mu_v + \nu_v)}\mathcal{R}_0$. □

3.5.2 Evaluation of Global Stability

This section presents a global stability analysis of the model, focusing on the disease-free equilibrium and the epidemic equilibrium points. We employed the Castillo-Chavez approach to investigate global stability at the DFE point (E_0), utilizing Lyapunov theory and LaSalle's invariance principle to examine global stability at the EE point (E_1).

To establish global stability at the DFE point (E_0), we employ the Castillo-Chavez approach, as described in [31]. This involves transforming the model into a suitable form, allowing us to apply this methodology and prove global stability. The model is reformulated in terms of two variables: $\mathcal{X} = (S_h, S_v)$, representing the susceptible individuals (mosquitoes and humans) who are not infected, $\mathcal{Y} = (E_h, I_h, A_h, E_v, I_v)$, representing the individuals (mosquitoes and humans) in various infection states. Thus, we have the following

reformulation of the model (3).

$$\begin{aligned} \frac{d\mathcal{X}}{dt} &= \mathcal{G}(\mathcal{X},\mathcal{Y}), \\ \frac{d\mathcal{Y}}{dt} &= \mathcal{L}(\mathcal{X},\mathcal{Y}), \quad \mathcal{Y}(\mathcal{G},0) = 0. \end{aligned} \tag{16}$$

Here, $\mathcal{X}$ represents the susceptible individuals as a scalar, while $\mathcal{Y}$ is a 5-dimensional vector representing the infected individuals in various states. Note that the recovered class is excluded from the analysis, as it does not interact with the other compartments and therefore does not influence the disease's dynamics. The DFE point is denoted as $E_0 = (\mathcal{X}_0, 0) = \left(\frac{\Lambda_h}{\mu h}, 0, 0, \frac{\Lambda_v}{\mu_v}, 0, 0, 0, 0\right)$. The following requirements are fulfilled to prove Global Asymptotic Stability (GAS) at the DFE point.

$$(G1) \quad \text{For } \frac{d\mathcal{X}}{dt} = \mathcal{G}(\mathcal{X},0) = 0,\ \mathcal{X}_0 \text{ is } GAS. \tag{17}$$

$$(G2) \quad \mathcal{L}(\mathcal{X},\mathcal{Y}) = \mathcal{B}\mathcal{Y} - \bar{\mathcal{L}}(\mathcal{X},\mathcal{Y}) \text{ where } \bar{\mathcal{L}}(\mathcal{X},\mathcal{Y}) \geq 0 \text{ for all } (\mathcal{X},\mathcal{Y}) \in \Delta. \tag{18}$$

Here, $\mathcal{B} = D_{\ddagger}\mathcal{L}(\mathcal{X}_0, 0)$ represents an M-matrix and Δ denotes the feasible region of the model. The following lemma can be derived, based on the work of Castillo-Chavez et al. [31].

Lemma 1: *If conditions G1 and G2 are met, the point $E_0 = (\mathcal{X}_0, 0)$ is globally asymptotically stable (GAS) when $\mathcal{R}_0 < 1$.*

Now, we proceed to confirm the following theorem.

Theorem 7: *The DFE point, E_0, is GAS whenever the number $\mathcal{R}_0 < 1$.*

Proof: We define $\mathcal{X} = (S_h, S_v)$ to represent the number of susceptible individuals, comprising humans (S_h) and mosquitoes (S_v). $\mathcal{Y} = (E_h, I_h, A_h, E_v, I_v)$ to represent the number of individuals in various infection states, including exposed humans (E_h), clinically infected humans (I_h), asymptomatic infected humans (A_h), exposed mosquitoes (E_v) and infected mosquitoes (I_v). The disease-free point, E_0, is represented by $E_0 = (\mathcal{X}_0, 0)$, where $\mathcal{X}_0$ denotes the number of susceptible individuals (both mosquitoes and humans) and zero represents the absence of infected individuals in all compartments. So

$$\frac{d\mathcal{X}}{dt} = \mathcal{G}(\mathcal{X}, Y) = \begin{bmatrix} \Lambda_h - \dfrac{\sigma b S_h I_v}{N_h} - \mu_h S_h \\ \Lambda_v - \dfrac{\sigma c S_v I_h}{N_h} - \mu_v S_v \end{bmatrix}. \tag{19}$$

If $S_h = S_{h0}$ and $S_v = S_{v0}$, then $\mathcal{G}(\mathcal{X}, 0) = 0$, i.e.,

$$\frac{d\mathcal{X}}{dt} = \begin{bmatrix} \Lambda_h - \mu_h S_h \\ \Lambda_v - \mu_v S_v \end{bmatrix}. \tag{20}$$

As $t \to \infty$, $\mathcal{X} \to \mathcal{X}_0$. Therefore, $\mathcal{X}_0 = (S_{h0}, S_{v0})$ is globally asymptotically stable.

Now,

$$\mathcal{B}\mathcal{Y} - \bar{\mathcal{L}}(\mathcal{X},\mathcal{Y}) = \begin{bmatrix} -k_1 & 0 & 0 & 0 & \frac{\sigma b S_{h0}}{N_h} \\ \beta_1 & -k_2 & 0 & 0 & 0 \\ \beta_2 & 0 & -k_3 & 0 & 0 \\ 0 & \frac{\sigma c S_{v0}}{N_h} & 0 & -k_4 & 0 \\ 0 & 0 & 0 & \nu_v & -\mu_v \end{bmatrix} \begin{bmatrix} E_h \\ I_h \\ A_h \\ E_v \\ I_v \end{bmatrix} - \begin{bmatrix} \Upsilon \\ 0 \\ \Pi \\ 0 \\ 0 \end{bmatrix}, \tag{21}$$

where, $\Upsilon = \frac{\sigma b I_v}{N_h}(S_{h0} - S_h)$ and $\Pi = \frac{\sigma c I_h}{N_h}(S_{v0} - S_v)$, and

$$\mathcal{B} = \begin{bmatrix} -k_1 & 0 & 0 & 0 & \frac{\sigma b S_{h0}}{N_h} \\ \beta_1 & -k_2 & 0 & 0 & 0 \\ \beta_2 & 0 & -k_3 & 0 & 0 \\ 0 & \frac{\sigma c S_{v0}}{N_h} & 0 & -k_4 & 0 \\ 0 & 0 & 0 & \nu_v & -\mu_v \end{bmatrix}, \quad \mathcal{Y} = \begin{bmatrix} E_h \\ I_h \\ A_h \\ E_v \\ I_v \end{bmatrix}, \quad \bar{\mathcal{L}}(\mathcal{X},\mathcal{Y}) = \begin{bmatrix} \Upsilon \\ 0 \\ \Pi \\ 0 \\ 0 \end{bmatrix}.$$

The matrix $\mathcal{B}$ is an M-matrix. As the equilibrium point is disease-free, we have $S_h \le S_{h0}$ and $S_v \le S_{v0}$, which implies that the matrix $\bar{\mathcal{L}}(\mathcal{X},\mathcal{Y}) \ge 0$. Therefore, the disease-free equilibrium point, E_0, is globally asymptotically stable. □

The following theorem illustrates the global stability of model (3) at the endemic equilibrium point E_1.

Theorem 8: *For disease model (3), if $\mathcal{R}_0 > 1$, the epidemic equilibrium point E_1 is globally asymptotically stable.*

Proof: A Volterra-type Lyapunov function is a powerful tool for establishing global stability. The function is defined as:

$$L(\Psi) = \left[S_h - S_h^1 - S_h^1 \log\frac{S_h}{S_h^1}\right] + \left[E_h - E_h^1 - E_h^1 \log\frac{E_h}{E_h^1}\right] + \left[I_h - I_h^1 - I_h^1 \log\frac{I_h}{I_h^1}\right] + \left[A_h - A_h^1 - A_h^1 \log\frac{A_h}{A_h^1}\right] + \left[R_h - Rh^1 - R_h^1 \log\frac{R_h}{R_h^1}\right] + \left[S_v - S_v^1 - S_v^1 \log\frac{S_v}{S_v^1}\right] + \left[E_v - E_v^1 - E_v^1 \log\frac{E_v}{E_v^1}\right] + \left[I_v - I_v^1 - I_v^1 \log\frac{I_v}{I_v^1}\right].$$

The equilibrium point $E_1 = (S_h^1, E_h^1, I_h^1, A_h^1, R_h^1, S_v^1, E_v^1, I_v^1)$ represents a state of equilibrium within the epidemic model. In terms of time t, we determine the following derivative of the Volterra-type Lyapunov function.

$$\frac{dL}{dt} = \left[\frac{dS_h}{dt} - \frac{S_h^1}{S_h}\frac{dS_h}{dt}\right] + \left[\frac{dE_h}{dt} - \frac{E_h^1}{E_h}\frac{dE_h}{dt}\right] + \left[\frac{dI_h}{dt} - \frac{I_h^1}{I_h}\frac{dI_h}{dt}\right] + \left[\frac{dA_h}{dt} - \frac{A_h^1}{A_h}\frac{dA_h}{dt}\right] + \left[\frac{dR_h}{dt} - \frac{R_h^1}{R_h}\frac{dR_h}{dt}\right] + \left[\frac{dS_v}{dt} - \frac{S_v^1}{S_v}\frac{dS_v}{dt}\right] + \left[\frac{dE_v}{dt} - \frac{E_v^1}{E_v}\frac{dE_v}{dt}\right] + \left[\frac{dI_v}{dt} - \frac{I_v^1}{I_v}\frac{dI_v}{dt}\right],$$

or

$$\frac{dL}{dt} = \left[\frac{S_h - S_h^1}{S_h}\right]\frac{dS_h}{dt} + \left[\frac{E_h - E_h^1}{E_h}\right]\frac{dE_h}{dt} + \left[\frac{I_h - I_h^1}{I_h}\right]\frac{dI_h}{dt} + \left[\frac{A_h - A_h^1}{A_h}\right]\frac{dA_h}{dt}$$

$$+\left[\frac{R_h - R_h^1}{R_h}\right]\frac{dR_h}{dt} + \left[\frac{S_v - S_v^1}{S_v}\right]\frac{dS_v}{dt} + \left[\frac{E_v - E_v^1}{E_v}\right]\frac{dE_v}{dt} + \left[\frac{I_v - I_v^1}{I_v}\right]\frac{dI_v}{dt}.$$

We substitute the derivatives in the equation with the right-hand side of the ODEs of the model (3), resulting in the following expression.

$$\begin{aligned}\frac{dL}{dt} &= \left[\frac{S_h - S_h^1}{S_h}\right]\left[\Lambda_h - \frac{\sigma b I_v S_h}{N_h} - \mu_h S_h\right] + \left[\frac{E_h - E_h^1}{E_h}\right]\left[\frac{\sigma b I_v S_h}{N_h} - (\beta_1 + \beta_2 + \mu_h)E_h\right] + \left[\frac{I_h - I_h^1}{I_h}\right] \\ &\times \left[\beta_1 E_h - (\theta + \mu_h + \delta_h)I_h\right] + \left[\frac{A_h - A_h^1}{A_h}\right]\left[\beta_2 E_h - (\mu_h + \gamma)A_h\right] + \left[\frac{R_h - R_h^1}{R_h}\right]\left[\theta I_h + \gamma A_h - \mu_h R_h\right] \\ &+ \left[\frac{S_v - S_v^1}{S_v}\right]\left[\Lambda_v - \frac{\sigma c I_h S_v}{N_h} - \mu_v S_v\right] + \left[\frac{E_v - E_v^1}{E_v}\right]\left[\frac{\sigma c I_h S_v}{N_h} - (\nu_v + \mu_v)E_v\right] + \left[\frac{I_v - I_v^1}{I_v}\right]\left[\nu_v E_v - \mu_v I_v\right].\end{aligned}$$

After rearranging the terms on the right-hand side, we obtain:

$$\begin{aligned}\frac{dL}{dt} =& \Bigg[\Lambda_h + (c_2 + \mu_h)\frac{(Sh^1)^2}{S_h} + c_2 S_h + k_1\frac{(Eh^1)^2}{Eh} + \beta_1 E_h + k_2\frac{(I_h^1)^2}{I_h} + \beta_2 E_h \\ &+ k_3\frac{(A_h^1)^2}{A_h} + (\mu_h)\frac{(R_h^1)^2}{R_h} + \theta I_h + \gamma A_h + \Lambda_v + (c_1 + \mu_v)\frac{(S_v^1)^2}{S_v} + c_1 S_v \\ &+ \nu_v E_v + \mu_v\frac{(I_v^1)^2}{I_v}\Bigg] - \Bigg[\Lambda_h\frac{S_h^1}{S_h} + (c_2 + \mu_h)\frac{(S_h - S_h^1)^2}{S_h} + (c_2 + \mu_h)S_h^1 \\ &+ c_2\frac{E_h^1}{E_h} + k_1\frac{(E_h - E_h^1)^2}{E_h} + k_1 E_h^1 + \beta_1 E_h\frac{I_h^1}{I_h} + k_2\frac{(I_h - I_h^1)^2}{I_h} + k_2 I_h^1 \\ &+ k_3\frac{(A_h - A_h^1)^2}{A_h} + \beta_2 E_h\frac{A_h^1}{A_h} + k_3 A_h^1 + \theta I_h\frac{R_h^1}{R_h} + \gamma A_h\frac{R_h^1}{R_h} + \mu_h\frac{(R_h - R_h^1)^2}{R_h} \\ &+ \mu_h R_h^1 + \Lambda_v\frac{S_v^1}{S_v} + (c_1 + \mu_v)\frac{(S_v - S_v^1)^2}{S_v} + (c_1 + \mu_v)S_v^1 + c_1\frac{E_v^1}{E_v} \\ &+ k_4\frac{(E_v^1)^2}{E_v} + k_4\frac{(E_v - E_v^1)^2}{E_v} + k_4 E_v^1 + \nu_v E_v\frac{I_v^1}{I_v} + \mu_v\frac{(I_v - Iv^1)^2}{I_v} + \mu_v I_v^1\Bigg].\end{aligned}$$

The above derivative expression for L can be rearranged to take the following form.

$$\frac{dL}{dt} = \Omega_1 - \Omega_2,$$

where

$$\begin{aligned}\Omega_1 =& \Bigg[\Lambda_h + (c_2 + \mu_h)\frac{(Sh^1)^2}{S_h} + c_2 S_h + k_1\frac{(Eh^1)^2}{Eh} + \beta_1 E_h + k_2\frac{(I_h^1)^2}{I_h} \\ &+ \beta_2 E_h + k_3\frac{(A_h^1)^2}{A_h} + (\mu_h)\frac{(R_h^1)^2}{R_h} + \theta I_h + \gamma A_h + \Lambda_v + (c_1 + \mu_v)\frac{(S_v^1)^2}{S_v} \\ &+ c_1 S_v + k_4\frac{(E_v^1)^2}{E_v} + \nu_v E_v + \mu_v\frac{(I_v^1)^2}{I_v}\Bigg],\end{aligned}$$

and

$$\Omega_2 = \Bigg[\Lambda_h \frac{S_h^1}{S_h} + (c_2+\mu_h)\frac{(S_h - S_h^1)^2}{S_h} + (c_2+\mu_h)S_h^1 + c_2\frac{E_h^1}{E_h} + k_1\frac{(E_h - E_h^1)^2}{E_h}$$
$$+ k_1 E_h^1 + \beta_1 E_h \frac{I_h^1}{I_h} + k_2\frac{(I_h - I_h^1)^2}{I_h} + k_2 I_h^1 + k_3\frac{(A_h - A_h^1)^2}{A_h} + \beta_2 E_h \frac{A_h^1}{A_h}$$
$$+ k_3 A_h^1 + \theta I_h \frac{R_h^1}{R_h} + \gamma A_h \frac{R_h^1}{R_h} + \mu_h \frac{(R_h - R_h^1)^2}{R_h} + \mu_h R_h^1 + \Lambda_v \frac{S_v^1}{S_v}$$
$$+ (c_1+\mu_v)\frac{(S_v - S_v^1)^2}{S_v} + (c_1+\mu_v)S_v^1 + c_1\frac{E_v^1}{E_v} + k_4\frac{(E_v - E_v^1)^2}{E_v} + k_4 E_v^1$$
$$+ \nu_v E_v \frac{I_v^1}{I_v} + \mu_v \frac{(I_v - Iv^1)^2}{I_v} + \mu_v I_v^1\Bigg].$$

Thus, $\frac{dL}{dt} < 0$ when $\Omega_1 < \Omega_2$ and $\frac{dL}{dt} = 0$ when $\Omega_1 = \Omega_2$. The case $\Omega_1 = \Omega_2$ implies that $S_h = S_h^1$, $E_h = E_h^1$, $I_h = I_h^1$, $A_h = A_h^1$, $R_h = R_h^1$, $S_v = S_v^1$, $E_v = E_v^1$, and $I_v = I_v^1$. Therefore, by LaSalle's Invariance Principle, the endemic point E_1 is GAS, meaning that all trajectories converge to E_1 as time approaches infinity, ensuring the long-term stability of the endemic state. □

Global stability means that the system converges to the endemic equilibrium point E_1 for any positive initial conditions, such as $t \to \infty$. Numerical evidence of global stability is shown in Fig. 2.

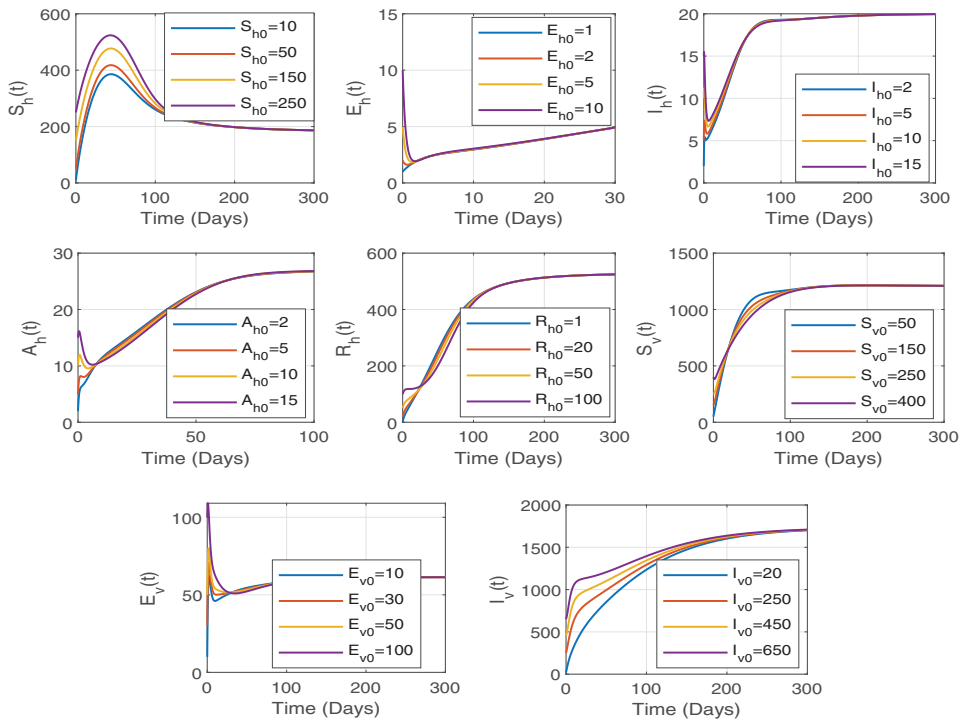

Figure 2: Figure displays the numerical evidence of global stability where the system trajectories converge to the endemic equilibrium point for any positive initial conditions

4 Sensitivity Analysis

Sensitivity analysis is crucial in formulating successful strategies to restrict or reduce the effect of a pandemic. Using sensitivity analysis tools, we can identify the parameters with the highest sensitivity to $\mathcal{R}_0$, which are essential for achieving our objectives. The ultimate goal is to reduce the transmission of the disease through interpersonal contact, thus lowering the value of reproduction $\mathcal{R}_0$ and reducing the risk of transmission.

The sensitivity of a parameter of the reproduction number $\mathcal{R}_0$ is determined by the sensitivity index, with a higher index value indicating a greater impact on $\mathcal{R}_0$. In other words, a higher sensitivity index means that small changes in the parameter will significantly affect $\mathcal{R}_0$, making it a crucial factor in controlling the spread of the disease. Utilizing the normalized sensitivity index [29], we do a sensitivity analysis using the formula:

$$S_\delta = \frac{\delta}{\mathcal{R}_0}\frac{\partial \mathcal{R}_0}{\partial \delta},$$

that gives the sensitivity index of the parameter δ. The sensitivity indices for each parameter of the reproduction number $\mathcal{R}_0$ are given in Table 2.

Table 2: Sensitivity indices of each of the parameter of $\mathcal{R}_0$

Transmission rates	Sensitivity index	Transmission rates	Sensitivity index
Λ_v	1	μ_h	0.9189726718
σ	1	β_1	0.5176418044
β_2	−0.5046895936	Λ_h	−1
θ	−0.47181	μ_v	−1
δ_h	−0.8427230046	c	1

The sensitivity indices in the given table provide valuable information about how modifications to certain parameters impact the reproduction number $\mathcal{R}_0$. Parameters with high positive sensitivity indices $(\Lambda_v,\ \sigma,\ c)$ have a direct impact on increasing the basic reproduction number $\mathcal{R}_0$. This implies that controlling or reducing these parameters, such as lowering transmission rates, would effectively decrease the number of reproductions and help restrict the spread of the disease. For example, a high sensitivity index value for σ suggests that variations in the rate at which humans contract vector infections have a substantial effect on $\mathcal{R}_0$. The sensitivity indices of μ_h and β_1 suggest that these parameters also play a significant role in determining $\mathcal{R}_0$. However, their impact is less prominent compared to σ and c. The presence of negative sensitivity indices for parameters $\beta_2,\ \theta,\ \mu_v,\ \Lambda_h,\ \delta_h$ suggests that an increase in these parameters would reduce the basic reproduction number $\mathcal{R}_0$. The vector mortality rate (μ_v) has the most significant negative impact, indicating that raising the vector mortality rate could be an effective strategy to reduce $\mathcal{R}_0$. The direct and indirect relationship of the parameters to $\mathcal{R}_0$ is shown in Fig. 3.

Therefore, implementing specific control strategies aimed at decreasing transmission rates (Λ_v), reducing susceptibility (σ), and improving vector mortality (μ_v) is likely to have the most substantial effect in reducing the basic number of reproduction $\mathcal{R}_0$.

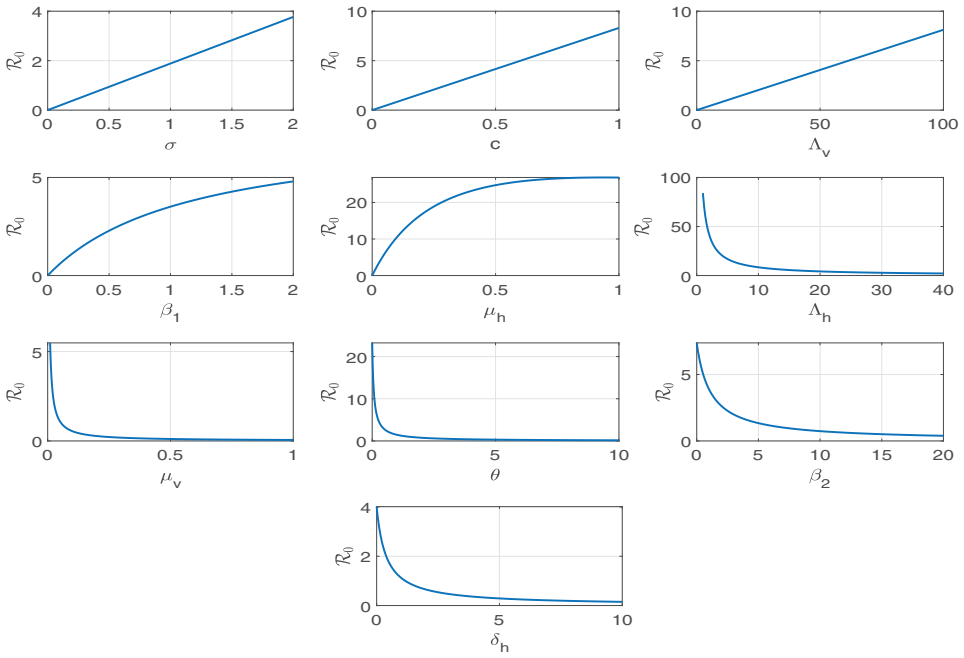

Figure 3: The parameters $\sigma, c, \Lambda_v, \beta_1, \mu_h$ have direct relationship to $\mathcal{R}_0$ whereas others have indirect relationship

5 Malaria Model for Disease Control

In this section, we extend the model outlined in (3) by adding a treat compartment T and adjusting three time-dependent control variables u_1, u_2, and u_3. These control variables are incorporated to denote different interventions intended to decrease the spread of the disease. The control variable u_1 represents efforts to reduce the transmission rate of the disease from infected humans to mosquitoes and vice versa. These efforts include interventions such as the use of insecticide-treated nets and indoor residual spraying, which decrease the likelihood of mosquito bites leading to infection. The variable u_2 is used to control the mosquito population by specifically targeting susceptible, exposed, and infected mosquito populations. It represents interventions such as larvicides, which reduce mosquito breeding, or other vector control measures that directly lower the mosquito population. The variable u_3 is dedicated to improving treatment rates within the human population, with a specific focus on improving the treatment of individuals in the treated class. This represents the administration of antimalarial drugs, rapid diagnostic testing, and other healthcare interventions that aim to effectively cure the infected population.

The revised system of ordinary differential equations with controls is presented as follows.

$$\frac{dS_h}{dt} = \Lambda_h - (1-u_1)\frac{\sigma b S_h I_v}{N_h} - \mu_h S_h, \tag{22a}$$

$$\frac{dE_h}{dt} = (1-u_1)\frac{\sigma b S_h I_v}{N_h} - (\beta_1 + \beta_2 + \mu_h)E_h, \tag{22b}$$

$$\frac{dI_h}{dt} = \beta_1 E_h - (\theta + \mu_h + \delta_h + \beta)I_h, \tag{22c}$$

$$\frac{dA_h}{dt} = \beta_2 E_h - (\mu_h + \gamma)A_h, \tag{22d}$$

$$\frac{dT_h}{dt} = \beta I_h - (\mu_h + \delta_1 + \rho)T_h - qu_3 T_h, \tag{22e}$$

$$\frac{dR_h}{dt} = \theta I_h + \gamma A_h + \rho T_h + qu_3 T_h - \mu_h R_h, \tag{22f}$$

$$\frac{dS_v}{dt} = \Lambda_v - (1-u_1)\frac{\sigma c S_v I_h}{N_h} - \mu_v S_v - pu_2 S_v, \tag{22g}$$

$$\frac{dE_v}{dt} = (1-u_1)\frac{\sigma c S_v I_h}{N_h} - (\nu_v + \mu_v)E_v - pu_2 E_v, \tag{22h}$$

$$\frac{dI_v}{dt} = \nu_v E_v - \mu_v I_v - pu_2 I_v, \tag{22i}$$

with initial conditions:

$$\begin{aligned} S_h(0) = S_{h0},\ E_h(0) = E_{h0},\ I_h(0) = I_{h0},\ A_h(0) = A_{h0},\ T_h(0) = T_{h0}, \\ R_h(0) = R_{h0},\ S_v(0) = S_{v0},\ E_v(0) = E_{v0},\ I_v(0) = I_{v0}, \end{aligned} \tag{22j}$$

where p represents the death rate of mosquitoes due to insecticides, q represents the rate of treatment among the population of humans, and the treated humans move to the recovered class at the rate ρ. Symptomatic infectious humans are treated at a rate β. The transmission dynamic of the disease across compartments is illustrated in Fig. 4.

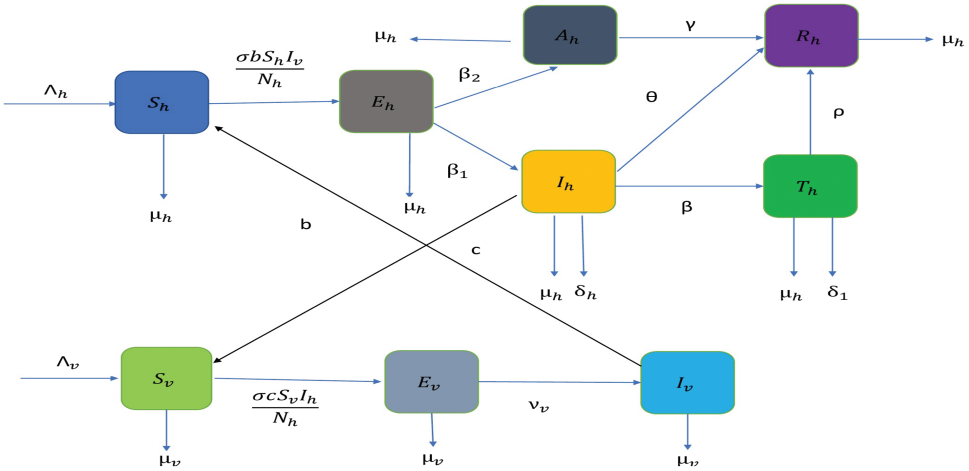

Figure 4: Flow diagram of an updated malaria model where we have incorporated a treatment compartment as a disease control strategy

5.1 Positive and Bounded Solutions

To demonstrate that the solutions of the malaria model (22) are positive and bounded for all $t \geq 0$, we present the following two theorems.

Theorem 9: *The solution* $\bar{\Psi}(t) = (S_h, E_h, I_h, A_h, T_h, R_h, S_v, E_v, I_v)$ *of the system (22) remains positive for all* $t \geq 0$.

Theorem 10: *The solution* $\bar{\Psi}(t) = (S_h, E_h, I_h, A_h, T_h, R_h, S_v, E_v, I_v)$ *of disease model (22) remains bounded* $\forall\, t \geq 0$.

The proof of these two theorems is similar to the proof of Theorems 1 and 2 presented for model (3).

5.2 Disease-Free Equilibrium Point and Reproduction Number

We solve the steady-state equations of the extended disease model (22) by considering $I_h = 0,\ A_h = 0,\ I_v = 0$ and determine the following disease-free equilibrium point.

$$\vec{E_0} = \left(\frac{\Lambda_h}{\mu_h}, 0, 0, 0, 0, 0, \frac{\Lambda_v}{\mu_v + pu_2}, 0, 0\right).$$

To derive the reproduction number for the modified malaria model (22), we divide the population into infected and uninfected compartments. The infected compartment includes individuals exposed to mosquitoes, infected mosquitoes, exposed humans, and those who are clinically and asymptomatically infected and have received treatment. All others are considered uninfected.

To determine $\mathcal{R}_0$, the next-generation matrix approach is employed. The Jacobian matrices F and V are computed at DFE point $\vec{E_0}$ by taking the derivatives of $\mathcal{F}$ and $\mathcal{V}$ with respect to the state variables $s = (E_h, I_h, A_h, T_h, E_v, I_v)$, i.e.,

$$F = \left(\frac{\partial \mathcal{F}_k}{\partial s_k}\right)_{\vec{E_0}} \quad \text{and} \quad V = \left(\frac{\partial \mathcal{V}_k}{\partial s_k}\right)_{\vec{E_0}} \quad k = 1, \ldots, 6,$$

where

$$\mathcal{F} = \begin{pmatrix} (1-u_1)\dfrac{\sigma b S_h I_v}{N_h} \\ 0 \\ 0 \\ 0 \\ (1-u_1)\dfrac{\sigma c S_v I_h}{N_h} \\ 0 \end{pmatrix}, \quad \mathcal{V} = \begin{pmatrix} (\beta_1 + \beta_2 + \mu_h)E_h \\ -\beta_1 E_h + (\theta + \mu_h + \delta_h + \beta)I_h \\ -\beta_2 E_h + (\mu + \gamma)A_h \\ -\beta I_h + (\mu_h + \delta_1 + \rho + qu_3)T_h \\ (\nu_v + \mu_v)E_v + pu_2 E_v \\ -\nu_v E_v + \mu_v I_v + pu_2 I_v \end{pmatrix}.$$

The spectral radius of the malaria transmission model is given by the maximum absolute value among the eigenvalues of FV^{-1}. This value represents a reproduction number, denoted by R_0. Therefore, the reproduction number of the malaria model (22) is determined by the spectral radius of FV^{-1}, which is calculated to give the following.

$$R_0 = \frac{(1-u_1)\sigma c \mu_h \Lambda_v \beta_1}{\Lambda_h(\mu_v + pu_2)(\beta_1 + \beta_2 + \mu_h)(\theta + \mu_h + \delta_h + \beta)}$$

The dynamics of the state variables, as shown in Fig. 5, illustrate two key scenarios based on the basic reproduction number, R_0. When $R_0 < 1$, the system's state variables converge towards the Disease-Free Equilibrium (DFE), indicating a decline in disease prevalence. Conversely, when $R_0 > 1$, the state variables tend to the endemic equilibrium point, suggesting that the disease stays within the population.

6 Optimal Control Problem

This section presents the most effective strategies to minimize the population's exposure to disease. It aims to prevent malaria through the use of mosquito nets, insecticides, and anti-malaria medications. By formulating an optimal control problem, we determine the optimal conditions necessary to achieve this goal [32–36].

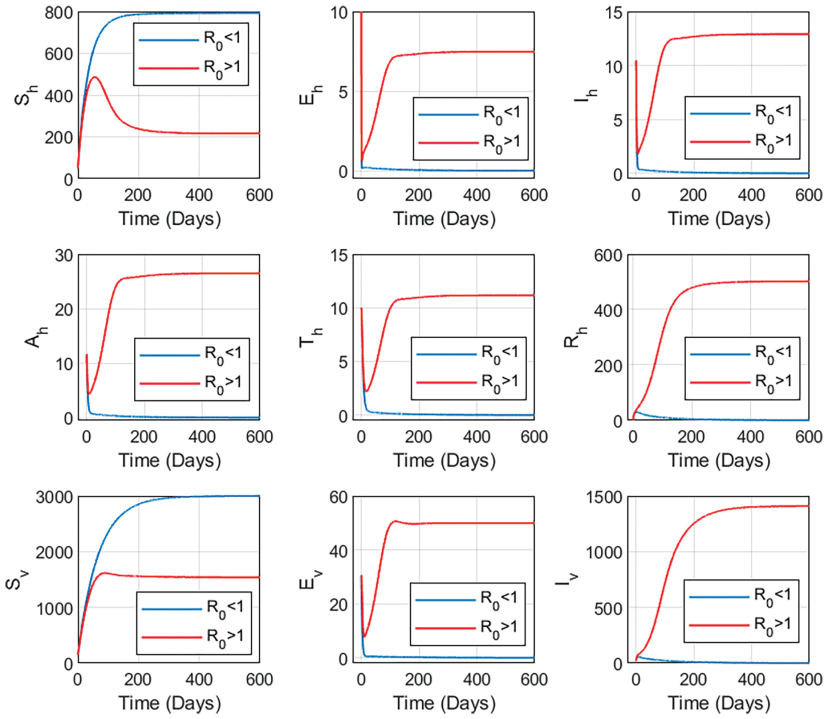

Figure 5: Figure illustrates two key scenarios based on the basic reproduction number, R_0. When $R_0 < 1$, the system's state variables converge towards the disease-free equilibrium (DFE). Conversely, when $R_0 > 1$, the state variables tend towards the endemic equilibrium (EE) point, suggesting that the disease stays within the population

6.1 Cost Functional

We consider the following cost functional to formulate an optimal control problem to implement disease control strategies.

$$J\left(\bar{\Psi}, u\right) = \int_0^{t_f} \left[E_h + I_h + T_h + E_v + I_v + \frac{1}{2}r_1 u_1^2(t) + \frac{1}{2}r_2 u_2^2(t) + \frac{1}{2}r_3 u_3^2(t)\right] dt. \tag{23}$$

In this context, t_f denotes the final time, $u(t) = (u_1, u_2, u_3)$ represents disease prevention controls: reducing disease transmission, controlling mosquito populations, improving the treatment, and r_1, r_2, r_3 signify the costs associated with these controls.

The objective is to minimize the cost functional (23), leading to determine the optimal control $u^* = (u_1^*, u_2^*, u_3^*) \in \bar{U}$, i.e.,

find $u^* \in \bar{U}$ that minimize $J(\bar{\Psi}, u)$ subject to constraints (22). (24)

$\bar{U}$ denotes the set of control variables defined as follows:

$$\bar{U} = \{u = (u_1, u_2, u_3) : \ 0 \le u_1, u_2, u_3 \le u_{max}, \ 0 \le t \le t_f\}.$$

6.2 Necessary Conditions

To derive the prerequisites for an effective control problem, Pontryagin's Maximum Principle is employed. The condition is expressed in terms of the Hamiltonian, $\mathcal{H}$, which is defined as follows.

$$\mathcal{H}(t, \bar{\Psi}, u, \eta) = \Theta(\bar{\Psi}, u) + \sum_{i=1}^{9} \eta_i g_i(t, \bar{\Psi}, u),$$

where $\Theta\left(\bar{\Psi}, u\right) = E_h + I_h + T_h + E_v + I_v + \frac{1}{2} r_1 u_1^2(t) + \frac{1}{2} r_2 u_2^2(t) + \frac{1}{2} r_3 u_3^2(t)$ and the system's dynamics is described by the variables $\bar{\Psi}$, while the associated adjoint variables are denoted by η_i, $i = 1, 2, 3, \ldots, 9$. To represent the right-hand side of the equations in the system (22), $g_i(t, \bar{\Psi}, u)$, where $i = 1, 2, 3, \ldots, 9$, is used. Consequently, the Hamiltonian for the problem can be expressed as:

$$\begin{aligned}
\mathcal{H}(t, \bar{\Psi}, u, \eta) = {} & E_h + I_h + T_h + E_v + I_v + \frac{1}{2} r_1 u_1^2(t) + \frac{1}{2} r_2 u_2^2(t) + \frac{1}{2} r_3 u_3^2(t) \\
& + \eta_1 \left(\Lambda_h - (1 - u_1) \frac{\sigma b S_h I_v}{N_h} - \mu_h S_h \right) \\
& + \eta_2 \left((1 - u_1) \frac{\sigma b S_h I_v}{N_h} - (\beta_1 + \beta_2 + \mu_h) E_h \right) \\
& + \eta_3 \left(\beta_1 E_h - (\theta + \mu_h + \delta_h + \beta) I_h \right) \\
& + \eta_4 \left(\beta_2 E_h - (\mu_h + \gamma) A_h \right) \\
& + \eta_5 \left(\beta I_h - (\mu_h + \delta_1 + \rho) T_h - q u_3 T_h \right) \\
& + \eta_6 \left(\theta I_h + \gamma A_h + \rho T_h - \mu_h R_h + q u_3 T_h \right) \\
& + \eta_7 \left(\Lambda_v - (1 - u_1) \frac{\sigma c S_v I_h}{N_h} - \mu_v S_v - p u_2 S_v \right) \\
& + \eta_8 \left((1 - u_1) \frac{\sigma c S_v I_h}{N_h} - (\nu_v + \mu_v) E_v - p u_2 E_v \right) \\
& + \eta_9 \left(\nu_v E_v - \mu_v I_v - p u_2 I_v \right).
\end{aligned}$$

The first optimality condition is met when

$$\frac{\partial \mathcal{H}}{\partial u} = 0,$$

which leads us to the following expressions for the control variables.

$$\begin{aligned}
u_1 &= \frac{\sigma b S_h I_v (\eta_2 - \eta_1) + \sigma c S_v I_h (\eta_8 - \eta_7)}{r_1 N_h}, \\
u_2 &= \frac{p(\eta_7 S_v + \eta_8 E_v + \eta_9 I_v)}{r_2}, \\
u_3 &= \frac{q T_h (\eta_5 - \eta_6)}{r_3}.
\end{aligned}$$

We impose bounds on control variables to ensure that the model remains realistic and feasible.

$$u_1^* = max \left\{ 0, min \left(u_{max}, \frac{\sigma b S_h I_v (\eta_2 - \eta_1) + \sigma c S_v I_h (\eta_8 - \eta_7)}{r_1 N_h} \right) \right\} \tag{25a}$$

$$u_2^* = max\left\{0, min\left(u_{max}, \frac{p(\eta_7 S_v + \eta_8 E_v + \eta_9 I_v)}{r_2}\right)\right\} \tag{25b}$$

$$u_3^* = max\left\{0, min\left(u_{max}, \frac{qT_h(\eta_5 - \eta_6)}{r_3}\right)\right\}. \tag{25c}$$

The second optimality condition:

$$\frac{d\eta_i}{dt} = -\frac{\partial \mathcal{H}}{\partial \bar{\Psi}_i}, \quad i = 1, 2, \ldots, 9,$$

results in an adjoint system of linear ordinary differential equations:

$$\frac{d\eta_1}{dt} = \left((1-u_1)\frac{\sigma b I_v}{N_h}\right)(\eta_1 - \eta_2) + \mu_h \eta_1, \tag{26a}$$

$$\frac{d\eta_2}{dt} = -1 + \beta_1(\eta_2 - \eta_3) + \beta_2(\eta_2 - \eta_4) + \mu_h \eta_2, \tag{26b}$$

$$\frac{d\eta_3}{dt} = -1 + \left((1-u_1)\frac{\sigma c S_v}{N_h}\right)(\eta_7 - \eta_8) + \theta(\eta_3 - \eta_6) + \beta(\eta_3 - \eta_5) + (\mu_h + \delta_h)\eta_3, \tag{26c}$$

$$\frac{d\eta_4}{dt} = \gamma(\eta_4 - \eta_6) + \mu_h \eta_4, \tag{26d}$$

$$\frac{d\eta_5}{dt} = -1 + \rho(\eta_5 - \eta_6) + (\mu_h + \delta_1)\eta_5 + qu_3(\eta_5 - \eta_6), \tag{26e}$$

$$\frac{d\eta_6}{dt} = \mu_h \eta_6, \tag{26f}$$

$$\frac{d\eta_7}{dt} = \left((1-u_1)\frac{\sigma c I_h}{N_h})\right)(\eta_7 - \eta_8) + (\mu_v + pu_2)\eta_7, \tag{26g}$$

$$\frac{d\eta_8}{dt} = -1 + \nu_v(\eta_8 - \eta_9) + (\mu_v + pu_2)\eta_8, \tag{26h}$$

$$\frac{d\eta_9}{dt} = -1 + \left((1-u_1)\frac{\sigma b S_h}{N_h}\right)(\eta_1 - \eta_2) + (\mu_v + pu_2)\eta_9, \tag{26i}$$

supported with the following terminal conditions:

$$\eta_i(t_f) = 0, \quad i = 1, 2, \ldots, 9. \tag{26j}$$

The derivative of $\mathcal{H}$ with regard to adjoint variables η_i, $i = 1, 2, \ldots, 9$ give us the state system (22).

Algorithm 1 outlines the procedure employed to derive an optimal solution $u^* = (u_1^*, u_2^*, u_3^*)$ for the control problem (24):

Algorithm 1: Steps to find the minimizer of the problem (24)

1. For $i = 0$, set initial control $u_i \in \bar{U}$.
2. Using the control u_i, estimate the state system (22) and the adjoint system (26a).
3. Utilizing the category of bounded controls (25), evaluate $u = (u_1, u_2, u_3)$.
4. Update the control u_i by using the formula $u_i = (u + u_i)/2$.
5. If the condition $\frac{\|\Phi_i - \Phi_{i-1}\|}{\|\Phi_i\|} < tolerance$ holds for $i > 0$, then **Exit**, otherwise $i \to i + 1$ and return to step 2.

With Φ standing in for all state variables, for adjoint variables, and the control variable.

6.3 Optimal Solutions and Discussions

In this section, we present a comprehensive analysis of the solutions to the optimal control problem outlined in Algorithm 1. The optimal solutions are obtained using the proposed algorithm along with its implementation in MATLAB. To discretize the state Eq. (22) and the adjoint Eq. (26a), we implement the Fourth-order Runge-Kutta (RK4) method. The continuous time domain $[0, t_f]$ is divided into N uniform subintervals with a positive width of $h = t_f/N$, which results in discrete time points $t_j = jh$ for $j = 0, 1, \ldots, N$. The state and adjoint variables are then approximated at these discrete time points. The cost functional (23) is evaluated numerically at the discrete points t_j by using Simpson's $\frac{1}{3}$ rule. To simulate the trajectories of the optimal control, the forward-backward sweep method is employed, following the approach detailed in [36].

In this analysis, three control variables are examined, and their impact on both the mosquito and human populations is illustrated through graphical representations. These visualizations highlight the influence of controls on disease dynamics and offer valuable insight into the effectiveness of the strategies implemented.

The profiles of the optimized control variables are illustrated in Fig. 6. It can be seen that all three controls begin at relatively high levels and then gradually decrease over time (days). At the beginning, a strong implementation of u_1 and u_2 is essential to rapidly reduce disease transmission and decrease mosquito population, respectively. Similarly, considerable effort is initially made through the control u_3 to improve treatment rates among the infected host population. As the burden of the disease declines over time, the intensity of the control efforts decreases. The lower panel of Fig. 6 shows the reduction of the cost functional J over successive iterations of the solution, demonstrating the successful convergence of the optimization algorithm. The significant drop in the value of the cost functional underscores the efficiency of the control strategy in alleviating both the health and economic burdens.

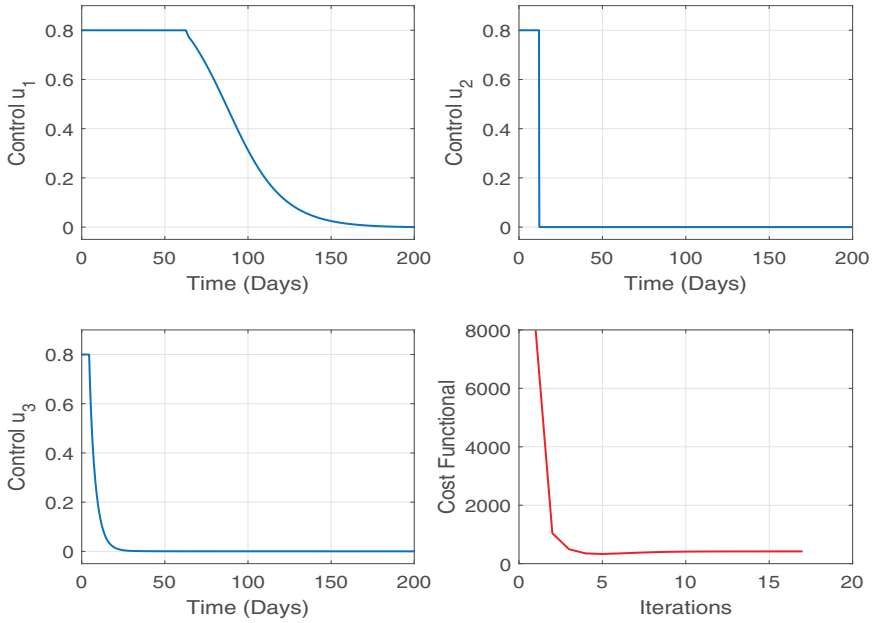

Figure 6: Figure shows the optimal profiles for control variables and their impact on the minimization of cost functional J. All three controls begin at relatively high levels and then gradually decrease over time. This means a strong implementation of u_1 and u_2 is essential to rapidly reduce disease transmission and to decrease the mosquito population

The effect of the optimal control strategy on the different compartments of the human population is depicted in Fig. 7. Without any control measures, the susceptible population decreases more significantly due

to the continuous spread of infections. However, with the implementation of the optimal control measures, a larger proportion of the human population remains susceptible, demonstrating effective disease prevention efforts. The number of people who are exposed, infected, asymptomatic, and receiving treatment is significantly decreased with controls than without, indicating a successful suppression of disease progression. In addition, we also observed a decrease in the recovered population with the optimal controls. The optimal profiles of the state variables suggest that the disease is progressing towards the disease-free state under the optimal control measures. These findings clearly highlight the positive effect of the control strategies on public health outcomes.

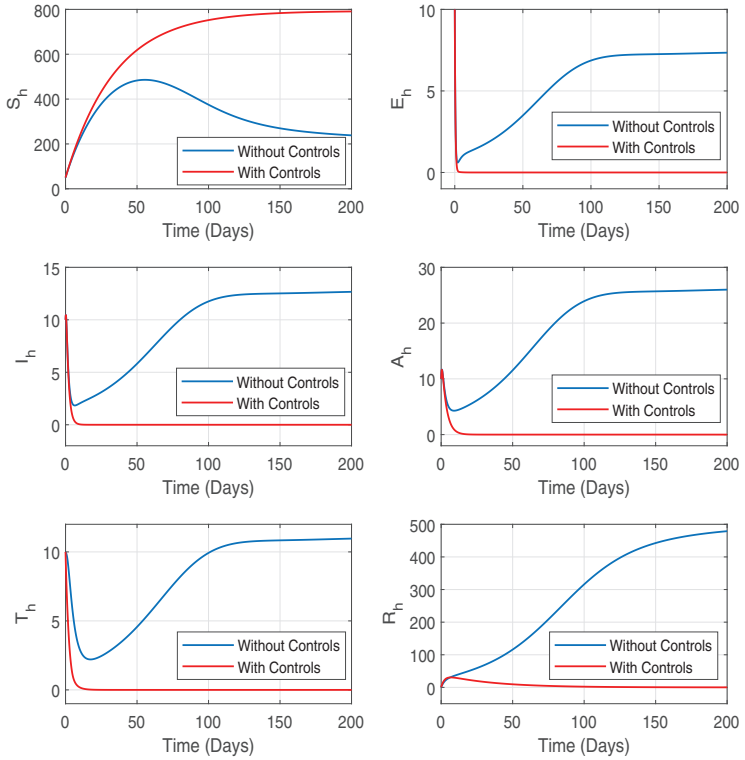

Figure 7: Figure shows the profile of state variables for the human population with and without optimal control variables. The convergence of trajectories of the optimal state variables E_h, I_h, A_h, T_h, R_h (red color) to zero shows that the disease is progressing towards a disease-free state under the optimal control measures

The impact of the control strategies on the mosquito population dynamics is illustrated in Fig. 8. The implementation of control measures results in a significant decrease in the population of susceptible, exposed, and infected mosquitoes compared to the uncontrolled scenario. Notably, the number of infected mosquitoes has observed a significant decline, which directly contributes to reducing the transmission of malaria to humans. These findings emphasize the critical role of mosquito control efforts, denoted by u_2, in the overall effectiveness of the malaria intervention strategies.

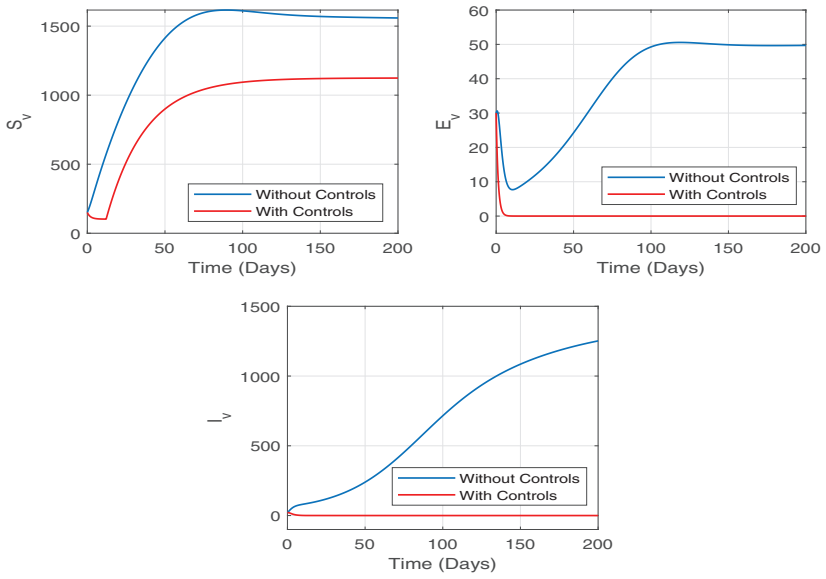

Figure 8: The impact of the control strategies on the mosquito population dynamics is illustrated in this Figure. We observe a significant decrease in the population of exposed and infected mosquitoes compared to the uncontrolled scenario

The graphical results illustrate the effectiveness and cost-efficiency of the optimal control strategy. By incorporating realistic intervention measures such as insecticide-treated nets, larvicides, and improved treatment protocols, the model accurately reflects the dynamics of the disease. The significant reduction in both disease prevalence and mosquito infection rates, achieved through moderate and gradually decreasing control measures, underscores the economic feasibility of the strategy. Furthermore, the decline in functional cost during the optimization process demonstrates that initial investments in intensive control measures can lead to substantial health improvements and long-term economic savings. In conclusion, the optimal control strategy suggested provides a valid and economically feasible method to manage and alleviate the burden of malaria.

7 Conclusions

The mathematical model developed in this study effectively captures the dynamics of malaria transmission. The model integrates asymptomatic human cases and vector populations into the traditional SEIR framework, providing a comprehensive understanding of the disease's transmission dynamics. Through a detailed stability analysis of disease-free and endemic equilibrium points, we have identified the critical role of the basic reproduction number (R_0) in determining the persistence or eradication of malaria. Our findings indicate that reducing (R_0) to less than one through strategic interventions is crucial to eradicating the disease. Furthermore, incorporating optimal control strategies, such as reducing mosquito populations, lowering transmission rates, and improving treatment, has shown significant potential to reduce the spread of malaria. Numerical simulations have verified that these strategies can effectively reduce infection rates while minimizing associated costs.

The study also underscores the importance of timely and coordinated interventions. Early implementation of control measures, such as insecticide-treated nets, indoor spraying, and antimalarial drug administration, leads to the most effective reduction in transmission. A cost-effectiveness analysis suggests that combining preventive and treatment measures results in sustainable long-term malaria control. This

model not only improves our understanding of the dynamics of malaria transmission but also provides practical strategies for public health authorities to implement and optimize malaria control efforts.

Some possible limitations of the model are the assumption that parameter values remain constant, the absence of spatial variability, and the exclusion of factors such as reinfection or partial immunity. Future research could introduce stochasticity and climate-related factors or different treatment regimens to further enhance its applicability in diverse settings.

Acknowledgement: We would like to thank the King Faisal University, The University of Tulsa and the University of Oklahoma for providing financial assistance.

Funding Statement: This work was supported by the Deanship of Scientific Research, Vice Presidency for Graduate Studies and Scientific Research, King Faisal University, Saudi Arabia [Grant No. KFU252959]. We are also thankful to The University of Tulsa and the University of Oklahoma for providing financial assistance.

Author Contributions: The authors confirm contribution to the paper as follows: Azhar Iqbal Kashif Butt: Conceptualization, Data curation, Formal analysis, Software, Validation, Writing—original draft, Project administration, resources. Tariq Ismaeel: Supervision, Data curation, Formal analysis, Investigation, Project administration, Resources, Writing—review & editing. Sara Khan: Conceptualization, Writing—original draft, Data curation, Formal analysis, Investigation. Muhammad Imran: Software, Validation, Visualization, Writing—review & editing. Waheed Ahmad: Formal analysis, Investigation, Validation, Visualization, Writing—review & editing. Ismail Abdulrashid: Data curation, Visualization, Project administration, Writing—review & editing. Muhammad Sajid Riaz: Software, Data curation, Project administration, Writing—review & editing. All authors reviewed the results and approved the final version of the manuscript.

Availability of Data and Materials: Data sharing not applicable to this article as no datasets were generated or analyzed during the current study.

Ethics Approval: Not applicable.

Conflicts of Interest: The authors declare no conflicts of interest to report regarding the present study.

Use of AI Tools Declaration The authors utilized ChatGPT AI to refine the language and enhance the clarity of this manuscript. All content was thoroughly reviewed and edited to ensure accuracy, and the authors take full responsibility for the final publication.

References

1. Haringo AT, Obsu LL, Bushu FK. A mathematical model of malaria transmission with media-awareness and treatment interventions. J Appl Math Comput. 2024;70(5):4715–53. doi:10.1007/s12190-024-02154-9.
2. Duve P, Charles S, Munyakazi J, Lühken R, Witbooi P. A mathematical model for malaria disease dynamics with vaccination and infected immigrants. Math Biosci Eng. 2024;21(1):1082–109. doi:10.3934/mbe.2024045.
3. Mojeeb A, Adu IK, Yang C. A simple SEIR mathematical model of malaria transmission. Asian Res J Math. 2017;7(3):1–22. doi:10.9734/arjom/2017/37471.
4. Imran M, McKinney BA, Butt AI, Palumbo P, Batool S, Aftab H. Optimal control strategies for dengue and malaria co-infection disease model. Mathematics. 2024;13(1):43. doi:10.3390/math13010043.
5. Crutcher JM, Hoffman SL. Malaria. In: Baron S, editor. Medical Microbiology. 4th edition. Galveston, TX, USA: University of Texas Medical Branch at Galveston; 1996.
6. White NJ. Determinants of relapse periodicity in Plasmodium vivax malaria. Malar J. 2011;10(1):297. doi:10.1186/1475-2875-10-297.

7. Yunus AO, Olayiwola MO. Mathematical modeling of malaria epidemic dynamics with enlightenment and therapy intervention using the Laplace-Adomian decomposition method and Caputo fractional order. Franklin Open. 2024;8(1):100147. doi:10.1016/j.fraope.2024.100147.
8. Yunus AO, Olayiwola MO. The analysis of a co-dynamic ebola and malaria transmission model using the Laplace Adomian decomposition method with Caputo fractional-order. Tanz J Sci. 2024;50(2):204–43. doi:10.4314/tjs.v50i2.5.
9. Abdulrashid I, Han X. A mathematical model of chemotherapy with variable infusion. Commun Pure Appl Anal. 2020;19(4):1875–90.
10. Abdulrashid I, Friji H, Topuz K, Ghazzai H, Delen D, Massoud Y. An analytical approach to evaluate the impact of age demographics in a pandemic. Stoch Environ Res Risk Assess. 2023;37(10):3691–705. doi:10.1007/s00477-023-02477-2.
11. Mandal S, Sarkar RR, Sinha S. Mathematical models of malaria—a review. Malar J. 2011;10(1):202. doi:10.1186/1475-2875-10-202.
12. Chiyaka C, Tchuenche JM, Garira W, Dube S. A mathematical analysis of the effects of control strategies on the transmission dynamics of malaria. Appl Math Comput. 2008;195(2):641–62. doi:10.1016/j.amc.2007.05.016.
13. Ngwa GA, Shu WS. A mathematical model for endemic malaria with variable human and mosquito populations. Math Comput Model. 2000;32(7–8):747–63. doi:10.1016/s0895-7177(00)00169-2.
14. Karaoglu S, Imran M, McKinney BA. Network-based SEITR epidemiological model with contact heterogeneity: comparison with homogeneous models for random, scale-free and small-world networks. Eur Phys J Plus. 2025;140(6):551. doi:10.1140/epjp/s13360-025-06481-z.
15. Ferraccioli F, Riccetti N, Fasano A, Mourelatos S, Kioutsioukis I, Stilianakis NI. Effects of climatic and environmental factors on mosquito population inferred from West Nile virus surveillance in Greece. Sci Rep. 2023;13(1):18803. doi:10.1038/s41598-023-45666-3.
16. Beck-Johnson LM, Nelson WA, Paaijmans KP, Read AF, Thomas MB, Bjørnstad ON. The effect of temperature on Anopheles mosquito population dynamics and the potential for malaria transmission. PLoS One. 2013;8(11):e79276. doi:10.1371/journal.pone.0079276.
17. Imran M, Butt AI, McKinney BA, Al Nuwairan M, Al Mukahal FH, Batool S. A comparative analysis of different fractional optimal control strategies to eradicate Bayoud disease in date palm trees. Fractal Fract. 2025;9(4):260. doi:10.3390/fractalfract9040260.
18. Yunus AO, Olayiwola MO. Epidemiological analysis of Lassa fever control using novel mathematical modeling and a dual-dosage vaccination approach. BMC Res Notes. 2025;18(1):199. doi:10.1186/s13104-025-07218-y.
19. Imran M, McKinney B, Butt AI. SEIR mathematical model for influenza-corona co-infection with treatment and hospitalization compartments and optimal control strategies. Comput Model Eng Sci. 2025;142(2):1899–931. doi:10.32604/cmes.2024.059552.
20. Srivastav AK, Steindorf V, Stollenwerk N, Aguiar M. The effects of public health measures on severe dengue cases: an optimal control approach. Chaos Solitons Fractals. 2023;172:113577.
21. Thongtha A, Modnak C. Optimal control strategy of a dengue epidemic dynamics with human-mosquito transmission. Bur Sci J. 2017;2017:333–42.
22. Adom-Konadu A, Yankson E, Naandam SM, Dwomoh D. A mathematical model for effective control and possible eradication of malaria. J Math. 2022;2022(1):6165581. doi:10.1155/2022/6165581.
23. Al Basir F, Abraha T. Mathematical modelling and optimal control of malaria using awareness-based interventions. Math. 2023;11(7):1687. doi:10.3390/math11071687.
24. Al-Arydah MT, Smith R. Controlling malaria with indoor residual spraying in spatially heterogenous environments. Math Biosci Eng. 2011;8(4):889–914. doi:10.3934/mbe.2011.8.889.
25. Traoré B, Sangaré B, Traoré S. A mathematical model of malaria transmission with structured vector population and seasonality. J Appl Math. 2017;2017(1):6754097. doi:10.1155/2017/6754097.
26. Moulay D, Aziz-Alaoui MA, Cadivel M. The chikungunya disease: modeling, vector and transmission global dynamics. Math Biosci. 2011;229(1):50–63. doi:10.1016/j.mbs.2010.10.008.
27. Burden R, Faires J. Numerical analysis. 9th ed. Boston, MA, USA: Cengage Learning; 2011.

28. Birkhoff G, Rota G. Ordinary differential equation. 4th ed. New York, NY, USA: John Wiley & Sons; 1989.
29. Van den Driessche P. Reproduction numbers of infectious disease models. Infect Dis Model. 2017;2(3):288–303. doi:10.1016/j.idm.2017.06.002.
30. Diekmann O, Heesterbeek JA, Metz JA. On the definition and the computation of the basic reproduction ratio R_0 in models for infectious diseases in heterogeneous populations. J Math Biol. 1990;28(4):365–82. doi:10.1007/bf00178324.
31. Castillo-Chavez C, Blower S, van den Driessche P, Kirschner D, Yakubu AA. Mathematical approaches for emerging and reemerging infectious diseases: models, methods, and theory. New York, NY, USA: Springer Science & Business Media; 2002.
32. Pontryagin LS. Mathematical theory of optimal processes. London, UK: Routledge; 2018.
33. Agusto FB. Optimal chemoprophylaxis and treatment control strategies of a tuberculosis transmission model. World J Model Simul. 2009;5(3):163–73.
34. Mukhtar AY, Munyakazi JB, Ouifki R, Clark AE. Modelling the effect of bednet coverage on malaria transmission in South Sudan. PLoS One. 2018;13(6):e0198280. doi:10.1371/journal.pone.0198280.
35. Imran M, Rafique H, Khan A, Malik T. A model of bi-mode transmission dynamics of Hepatitis C with optimal control. Theory in Biosciences. 2014;133(2):91–109. doi:10.1007/s12064-013-0197-0.
36. Lenhart S, Workman JT. Optimal control applied to biological models. Boca Raton, FL, USA: Chapman and Hall/CRC; 2007.